

VAND-TH-94-25
 SHEP 95-02
 January 1995

Radiative Corrections to Charged Higgs Production in e^+e^- Colliders*

Marco A. Díaz

*Physics Department, University of Southampton
 Southampton, SO17 1BJ, U.K.*

and

Tonnis A. ter Veldhuis
*Department of Physics and Astronomy, Vanderbilt University
 Nashville, TN 37235, USA*

Abstract

We study one loop electroweak corrections to the production of a pair of charged Higgs bosons through an intermediate Z -boson or photon. In particular, we consider the effects of graphs with top and bottom quarks and squarks in the loop within the context of the Minimal Supersymmetric Model. We find that the corrections can be considerable, and typically are of the order of 10% to 20%.

*Presented by Tonnis ter Veldhuis at the Eighth Meeting of the Division of Particles and Fields of the American Physical Society “DPF94”, The University of New Mexico, Albuquerque, August 2-6, 1994, and at “Beyond the Standard Model IV”, Granlibakken, Lake Tahoe, December 13-18, 1994.

The minimal supersymmetric standard model (MSSM) [1] provides a very interesting extension of the standard model. The absence of quadratic divergencies in this model is an immediate consequence of its supersymmetric nature. The ensuing improved UV behavior ameliorates the technical aspect of the naturalness problem that haunts the standard model (SM). Furthermore, it is tempting to believe that the unification of the gauge coupling constants is not coincidental [2]; the required SUSY breaking scale is small enough to avoid the reintroduction of the naturalness problem, and the unification scale is large enough to suppress proton decay yet smaller than the Planck scale. Indeed, a supergravity theory with non-perturbative SUSY breaking may even explain the hierarchy of energy scales.

The Higgs sector of the MSSM contains two neutral Higgs bosons, a pseudo scalar Higgs boson, and a pair of charged Higgs bosons [3]. The next generation of e^+e^- colliders, notably LEP2 and the NLC, will be able to probe the MSSM Higgs sector and test the model. It is therefore important to understand the production and decay of charged Higgs bosons in detail.

Radiative corrections in the MSSM can be considerable because of the large mass splitting between the top and bottom quark. For instance, the tree-level upper bound on the lightest Higgs mass is M_Z , but radiative corrections increase this upper bound to 130 GeV [4]. Here we study the one-loop electroweak corrections to the production cross-section of a pair of charged Higgs bosons in e^+e^- colliders.

We work in an on-shell scheme [5], in which $M_Z^2 = 1/4(g^2 + g'^2)v^2$ and $M_W^2 = 1/4g^2v^2$, with $v^2 = v_t^2 + v_b^2$, are defined to be the physical masses of the vector bosons. Similarly, we define the tree-level expression for the mass of the pseudoscalar in terms of the renormalized parameters to be the physical mass. The residues of the poles of the photon and the pseudoscalar propagators are equal to one in our scheme, and the mixing between the photon and the Z boson vanishes at zero momentum. The normalization conditions that complete the set relevant to this paper are imposed on the coupling of the pseudoscalar to charged leptons

$$\Gamma_{A l^+ l^-} |_{p^2=M_A^2} = -\frac{g m_l \tan \beta}{2 M_W}, \quad (1)$$

and the coupling of the photon to electrons

$$\Gamma_{\gamma e^+ e^-}^\mu |_{p^2=0} = ie\gamma^\mu. \quad (2)$$

The angles θ_W and β are defined by $\sin^2 \theta_W = 1 - M_W^2/M_Z^2$ and $\tan \beta = v_b/v_t$, and the electric charge is $e = gg'/\sqrt{g^2 + g'^2}$.

We consider the production of a pair of on-shell charged Higgs bosons. The momenta k_μ and k'_μ of the outgoing charged Higgs bosons therefore satisfy $k^2 = k'^2 = M_{H^\pm}^2$. The amplitude for the process is given by

$$I = -\frac{g^2 \cos 2\theta_W}{4 \cos^2 \theta_W} \bar{v}_{p_2} \gamma_\mu (v_z - a_z \gamma_5) u_{p_1} \frac{g^{\mu\nu}}{p^2 - M_Z^2} (f_Z k_\nu - f'_Z k'_\nu) - e^2 \bar{v}_{p_2} \gamma_\mu (v_\gamma - a_\gamma \gamma_5) u_{p_1} \frac{g^{\mu\nu}}{p^2} (f_\gamma k_\nu - f'_\gamma k'_\nu). \quad (3)$$

Here $v_z = 1/2 - 2 \sin^2 \theta_W$, $a_z = 1/2$, $v_\gamma = 1$ and $a_\gamma = 0$. The form factors f_Z , f'_Z , f_γ and f'_γ are equal to one at tree-level. Radiative corrections manifest themselves in modifications of these form factors

$$\begin{aligned} f_Z &= 1 + \frac{\tilde{A}_{ZZ}}{p^2 - M_Z^2} + \tan 2\theta_W \frac{\tilde{A}_{\gamma Z}}{p^2} + \tilde{A}_{ZH^+H^-} + \tilde{A}_{H^+H^-}^d(M_{H^\pm}), \\ f'_Z &= 1 + \frac{\tilde{A}_{ZZ}}{p^2 - M_Z^2} + \tan 2\theta_W \frac{\tilde{A}_{\gamma Z}}{p^2} + \tilde{A}'_{ZH^+H^-} + \tilde{A}_{H^+H^-}^d(M_{H^\pm}), \\ f_\gamma &= 1 + \frac{\tilde{A}_{\gamma\gamma}}{p^2} + \frac{1}{\tan 2\theta_W} \frac{\tilde{A}_{Z\gamma}}{p^2 - M_Z^2} + \tilde{A}_{\gamma H^+H^-} + \tilde{A}_{H^+H^-}^d(M_{H^\pm}), \\ f'_\gamma &= 1 + \frac{\tilde{A}_{\gamma\gamma}}{p^2} + \frac{1}{\tan 2\theta_W} \frac{\tilde{A}_{Z\gamma}}{p^2 - M_Z^2} + \tilde{A}'_{\gamma H^+H^-} + \tilde{A}_{H^+H^-}^d(M_{H^\pm}), \end{aligned} \quad (4)$$

where the tilde indicates renormalized quantities with infinities subtracted in accordance with the normalization conditions. The various terms in the modified form factors are related to the gauge boson self-energies, $\tilde{\Pi}_{ij}^{\mu\nu} = i\tilde{A}_{ij}g^{\mu\nu} + i\tilde{B}_{ij}p^\mu p^\nu$ with $i, j = \gamma, Z$, to the loop contributions of the vertices, $\tilde{\Lambda}_{ZH^+H^-}^\mu = i\tilde{A}_{ZH^+H^-}k^\mu - i\tilde{A}'_{ZH^+H^-}k'^\mu$ and $\tilde{\Lambda}_{\gamma H^+H^-}^\mu = \tilde{A}_{\gamma H^+H^-}k^\mu - \tilde{A}'_{\gamma H^+H^-}k'^\mu$, and to the charged Higgs boson self-energy, $i\tilde{A}_{H^+H^-}^d = \frac{d}{dp^2}\tilde{\Sigma}_{H^+H^-}$. We calculate one-loop oblique and vertex corrections. As large radiative corrections are expected to arise from the high value of the top quark mass, we furthermore limit our calculation to loops with top and bottom quarks, and with stop and sbottom squarks. In this approximation there are no contributions from box diagrams. The differential cross-section therefore has the characteristic $\sin^2 \theta$ scattering angle dependence of s-channel processes. The total cross-section in terms of the form factors is

$$\begin{aligned} \sigma &= \frac{(1 - 4M_{H^\pm}/s)^{\frac{3}{2}}}{48\pi s} \left\{ \frac{g^4 \cos^2 2\theta_w}{16 \cos^4 \theta_w} \frac{v_z^2 + a_z^2}{(1 - M_Z^2/s)^2} \left| \frac{f_Z + f'_Z}{2} \right|^2 + \right. \\ &\quad \left. e^4 \left| \frac{f_\gamma + f'_\gamma}{2} \right|^2 + 2 \frac{g^2 \cos 2\theta_w}{4 \cos^2 \theta_w} e^2 \frac{v_z}{(1 - M_Z^2/s)} \Re \left[\left(\frac{f_Z + f'_Z}{2} \right) \left(\frac{f_\gamma + f'_\gamma}{2} \right)^* \right] \right\} \end{aligned} \quad (5)$$

where \sqrt{s} is the center of mass energy, and M_{H^\pm} is the renormalized charged Higgs boson mass [6].

Radiative corrections enter the total cross-section both through corrections to the charged Higgs boson mass M_{H^\pm} and through corrections to the form factors. Corrections to the charged higgs boson mass M_{H^\pm} manifest themselves in the fact that the tree-level mass relation $M_{H^\pm}^2 = M_W^2 + M_A^2$ is not longer valid. As shown in Fig. 1, departures from this mass relation are most pronounced for very small and very large values of $\tan \beta$.

In Fig. 2a we plot the total cross-section as a function of the center of mass energy \sqrt{s} for various values of $\tan \beta$ and the pseudoscalar mass M_A . We plot the tree-level cross-section (dashed lines) and the cross-section including all one-loop corrections (solid lines) within our approximations. All soft SUSY breaking squark mass parameters are equal to $M_{SUSY} = 400 \text{ GeV}$, and the Peccei-Quinn symmetry breaking parameter μ as well as the soft SUSY breaking trilinear couplings are taken to be zero, a choice that implies no mixing in the squark sector. The top quark mass is taken to be $m_t = 174 \text{ GeV}$, the central value of the recent CDF result [7]. Because the curves in Fig. 2a reflect a fixed value of the pseudoscalar higgs boson mass M_A , radiative corrections to the charged Higgs boson mass cause a shift in the production threshold; to lower \sqrt{s} for low values of $\tan \beta$, and to higher \sqrt{s} for high values of $\tan \beta$. For intermediate values of $\tan \beta$ the dashed and the dot-dashed curves almost coincide, even near threshold, reflecting the negligible radiative corrections to the charged Higgs boson mass in this range. The solid curve corresponding to $\tan \beta = 0.5$ has a discontinuity in slope at $\sqrt{s} = 2m_t = 348 \text{ GeV}$. This discontinuity stems from the triangular graph with two top quarks and a bottom quark in the internal lines, and its effect is enhanced at low values of $\tan \beta$. In Fig. 2b we again show the cross-section as a function of the center of mass energy \sqrt{s} , but now for fixed values of the charged higgs boson mass M_{H^\pm} . Accordingly the production threshold at tree-level (dashed line) and the at one loop (solid line) coincide, but the values of the pseudoscalar higgs mass M_A at tree and one-loop level differ. For center of mass energies well above threshold, the solid lines show that for our choice of parameters one-loop corrections to the form factors reduce the cross-section by 10% to 25% with respect to the tree-level cross-section. .

In Fig. 3 we plot the ratio between the one-loop renormalized cross section and the tree level cross section, as a function of $\tan \beta$ for various values of the top quark mass for fixed values of the pseudoscalar mass M_A (dashed lines). To separate the effect of the corrections to the charged Higgs mass, we plot the ratio between the one-loop renormalized cross section and the cross section with corrected M_{H^\pm} , but form factors

equal to one (solid lines). Solid and dashed lines coincide at intermediate values of $\tan \beta$ because in that region the corrections to the charged Higgs mass are negligible, as can be seen in Fig. 1, where the renormalized charged Higgs mass is shown as a function of $\tan \beta$ for the same values of the top quark mass. We appreciate from Fig. 3 that the corrections to the cross section are typically between -10% to -20% in the intermediate region of $\tan \beta$ for our choice of parameters. For more extreme values of $\tan \beta$ corrections can be larger and can have either sign. These large corrections stem mainly from corrections to the form factors.

Note: While we were completing this work we received a preprint concerning a similar calculation [8].

References

- [1] H.P. Nilles, *Phys. Rep.* **110**, 1 (1984); H.E. Haber and G.L. Kane, *Phys. Rep.* **117**, 75 (1985); R. Barbieri, *Riv. Nuovo Cimento* **11**, 1 (1988).
- [2] M.B. Einhorn and D.T.R. Jones, *Nucl. Phys.* **B196**, 475 (1982); W.. Marciano and G. Senjanovic, *Phys. Rev. D* **25**, 3092 (1982); U. Amaldi et al. , *Phys. Rev. D* **36**, 1385 (1987); U. Amaldi et al. , *Phys. Lett. B* **260**, 447 (1991); U. Amaldi et al. , *Phys. Lett. B* **281**, 374 (1992).
- [3] J.F. Gunion, H.E. Haber, G. Kane, and S. Dawson, *The Higgs Hunter's Guide* (Addison-Wesley Publishing Company, Redwood City, CA, 1990).
- [4] M.S. Berger, *Phys. Rev. D* **41**, 225 (1990); H.E. Haber and R. Hempfling, *Phys. Rev. Lett.* **66**, 1815 (1991); Y. Okada M. Yamaguchi and T. Yanagida, *Prog. Theor. Phys.* **85**, 1 (1991); J. Ellis G. Ridolfi and F. Zwirner, *Phys. Lett. B* **257**, 83 (1991); R. Barbieri M. Frigeni, F. Caravaglios, *Phys. Lett. B* **258**, 167 (1991); Y. Okada M. Yamaguchi and T. Yanagida, *Phys. Lett. B* **262**, 54 (1991); J.R. Espinosa and M. Quirós, *Phys. Lett. B* **266**, 389 (1991); A. Yamada, *Phys. Lett. B* **263**, 233 (1991); J. Ellis G. Ridolfi and F. Zwirner, *Phys. Lett. B* **262**, 477 (1991); M. Drees and M.M. Nojiri, *Phys. Rev. D* **45**, 2482 (1992); R. Barbieri and M. Frigeni, *Phys. Lett. B* **258**, 395 (1991); A. Brignole, *Phys. Lett. B* **281**, 284 (1992); M.A. Díaz and H.E. Haber, *Phys. Rev. D* **46**, 3086 (1992).
- [5] M.A. Díaz, *Phys. Rev. D* **48** (1993) 2152.

- [6] J.F. Gunion and A. Turski, *Phys. Rev. D* **39**, 2701 (1989); **40**, 2333 (1989); A. Brignole ,J. Ellis, G. Ridolfi, and F. Zwirner, *Phys. Lett. B* **271**, 123 (1991); M. Drees and M.M. Nojiri, *Phys. Rev. D* **45**, 2482 (1992); A. Brignole, *Phys. Lett. B* **277**, 313 (1992); P.H. Chankowski , S. Pokorski, and J. Rosiek, *Phys. Lett. B* **274**, 191 (1992); M.A. Díaz and H.E. Haber, *Phys. Rev. D* **45**, 4246 (1992).
- [7] F. Abe et al. CDF Collaboration, Fermilab Pub-94/097-E, (1994).
- [8] A. Arhrib, M. Capdequi-Peyranère and G. Mourtaka, **SLAC-PUB-6529, PM/94-17**.

Figure Captions:

Fig. 1. Renormalized charged Higgs mass as a function of $\tan \beta$ for different values of the top quark mass. In solid we plot the CDF central value $m_t = 174$ GeV. In dashes we have the 1σ deviations from the central value: $m_t = 158$ and 190 GeV. In dotdashes we plot the 95% c.l. lower limit $m_t = 131$ GeV. The horizontal dotted line corresponds to the tree level charged Higgs mass.

Fig. 2a. The cross-section $\sigma(e^+e^- \rightarrow H^+H^-)$, as a function of the center of mass energy \sqrt{s} for fixed values of M_A . Dashed (solid) lines show the tree-level (one-loop) result.

Fig. 2b. The cross-section $\sigma(e^+e^- \rightarrow H^+H^-)$, as a function of the center of mass energy \sqrt{s} for fixed values of M_{H^\pm} . Dashed (solid) lines show the tree-level (one-loop) result.

Fig. 3. Ratio between the one-loop renormalized cross section and the tree level cross section as a function of $\tan \beta$ for different values of the top quark mass (dashed lines). For comparison we also plot the ratio between the one-loop renormalized cross section and the cross section with corrected charged Higgs mass but form factors equal to one (solid lines).

This figure "fig1-1.png" is available in "png" format from:

<http://arxiv.org/ps/hep-ph/9501315v1>

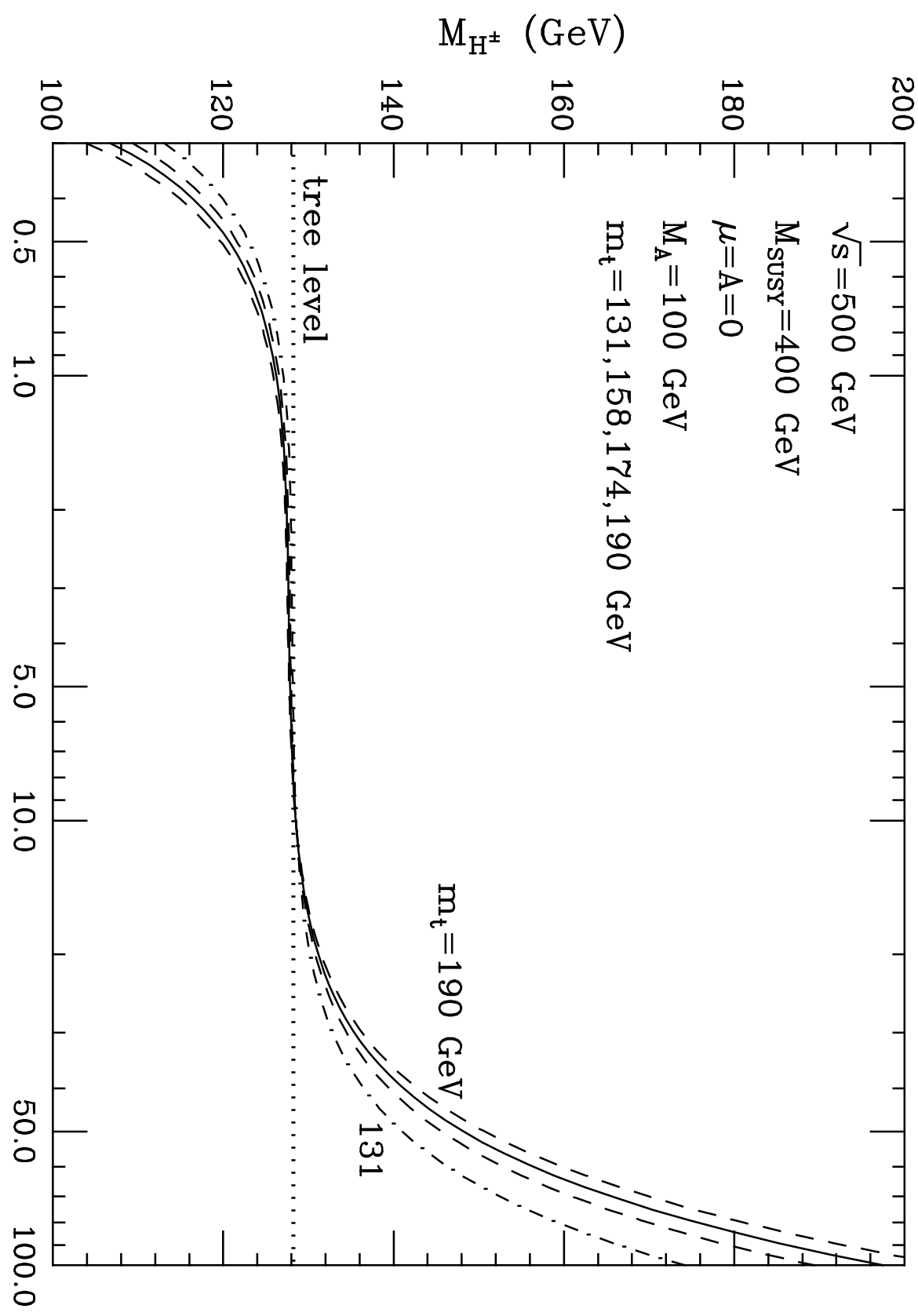
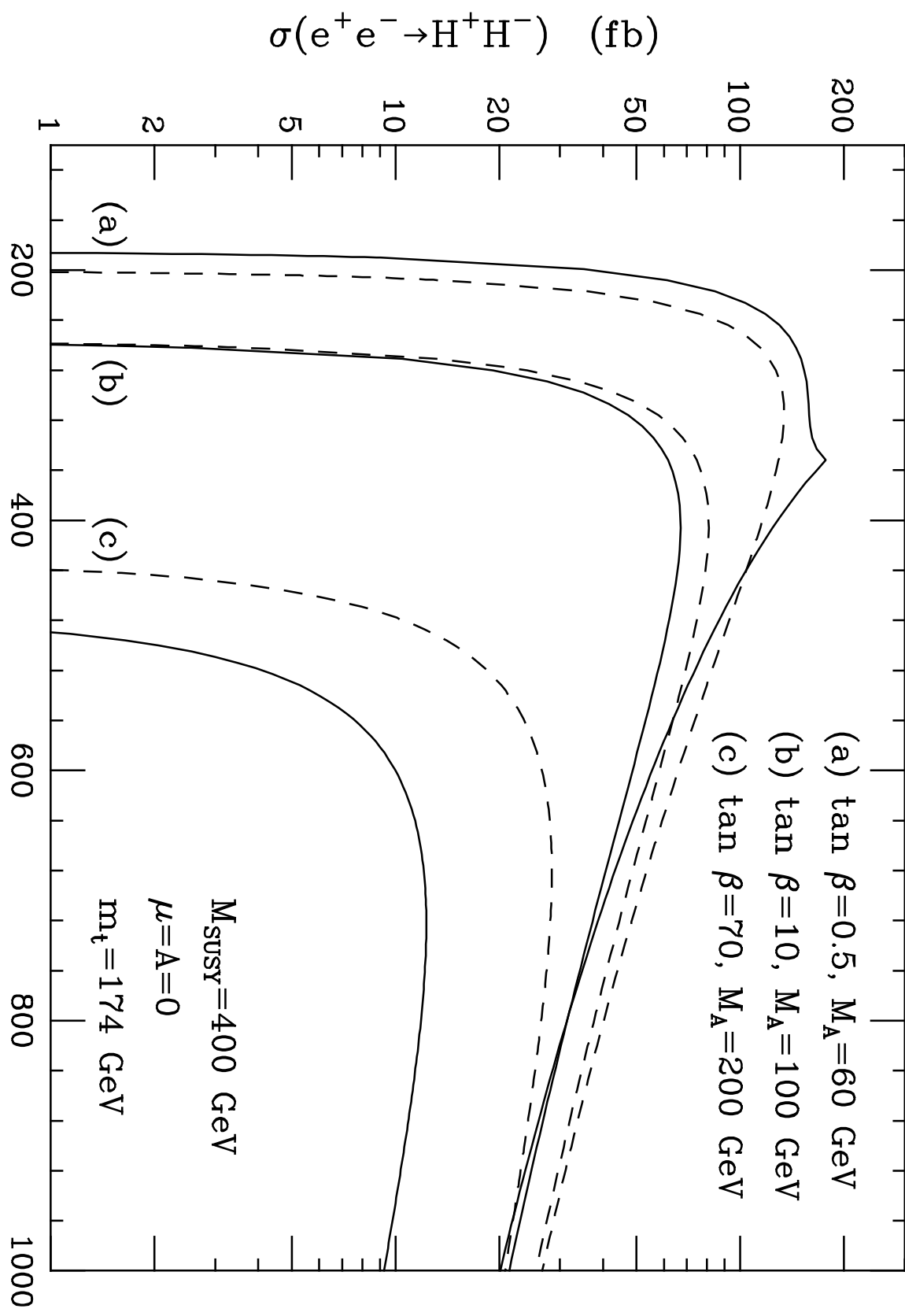


Fig. 1

This figure "fig1-2.png" is available in "png" format from:

<http://arxiv.org/ps/hep-ph/9501315v1>

Fig. 2a



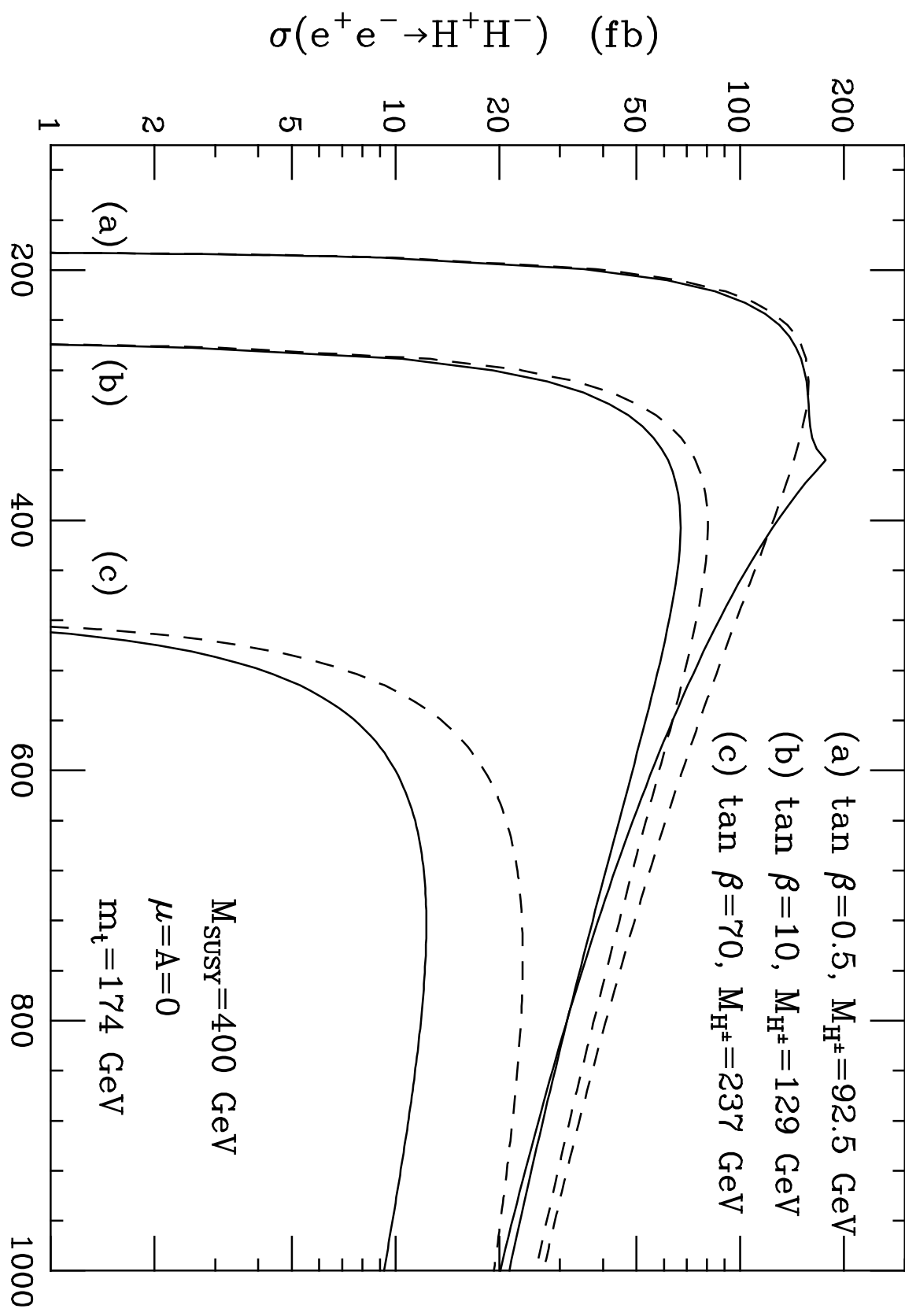


Fig. 2b

This figure "fig1-3.png" is available in "png" format from:

<http://arxiv.org/ps/hep-ph/9501315v1>

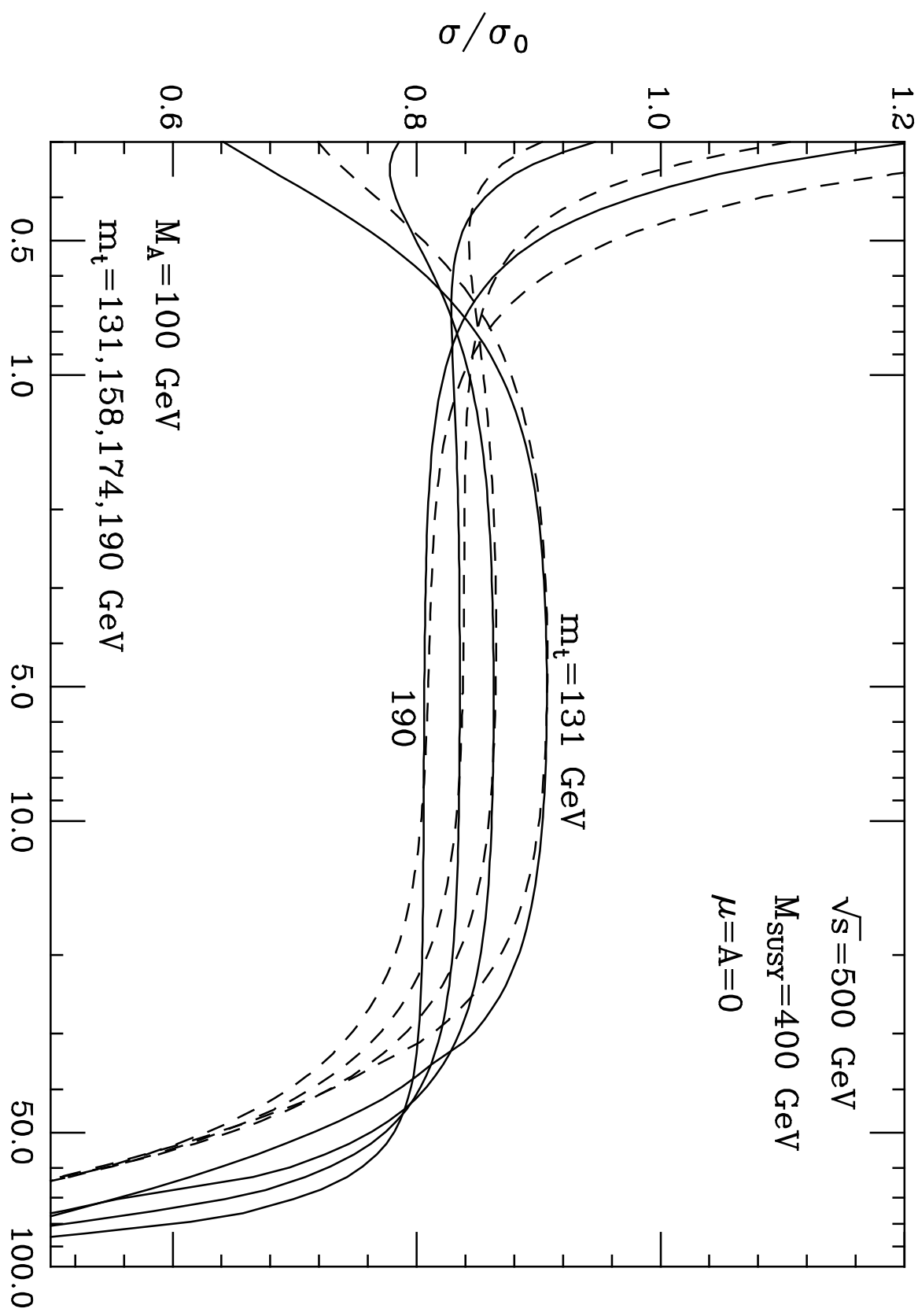


Fig. 3

This figure "fig1-4.png" is available in "png" format from:

<http://arxiv.org/ps/hep-ph/9501315v1>